REDUCTION OF CROSSED-FIELD DIODE TRANSMITTED CURRENT DUE TO ANODE SECONDARY EMISSION

by

V. P. Gopinath and Bo Vanderberg

Memorandum No. UCB/ERL M97/23

15 April 1997

REDUCTION OF CROSSED-FIELD DIODE TRANSMITTED CURRENT DUE TO ANODE SECONDARY EMISSION

by

V. P. Gopinath and Bo Vanderberg

Memorandum No. UCB/ERL M97/23

15 April 1997

ELECTRONICS RESEARCH LABORATORY

College of Engineering
University of California, Berkeley
94720

Reduction of Crossed-field Diode Transmitted Current due to Anode Secondary Emission

V. P. Gopinath
EECS Department, University of California, Berkeley, CA 94720

Bo Vanderberg
Uppsala University, Uppsala, Sweden

Abstract

The limiting current theory for planar crossed-field diodes has long been studied extensively for various emission energies and temperatures. However, experimental measurements of transmitted current have shown significant departure from theory. This paper attempts to explain the reduction in transmitted current from theory in terms of secondary electron emission created by electrons hitting the anode. This paper proposes that the presence of the secondary electrons increases the charge density in the gap, thereby reducing the amount of current transmitted. A detailed secondary emission model is implemented in a particle–in–cell code to study current reduction. The effect of secondary electrons on charge density, and on the resultant electric field and potential is also presented.

1 Background

Currents in planar crossed-field diodes have been analytically and experimentally studied for over 70 years [1]- [6] for $B < B_{Hull}$. Recently simulations have been done [7] for warm electron emissions which confirm the limiting currents predicted by [4]. However, theories and simulations have regularly neglected the effect of secondary electrons created at the anode by the high energy primaries. Typically, in the absence of any collisions, an electron emitted from the cathode gains kinetic energy close to the gap voltage as it approaches the anode. Experimental measurements of limiting current in crossed-field diodes by Vanderberg and Eninger [8] and Pollack [5] have shown that the measured values of transmitted currents are significantly less than the theoretically predicted limits. Their studies also showed a larger decrease in limiting current for higher magnetic fields, implying

(indirectly) a strong effect due to the higher angle of incidence of incident electrons (i.e. values of B closer to B_H). Recent studies by Verboncoeur *et al.* [7] have shown that even a small ($< 1\%$) over–injection of current pushes the diode from a laminar, 100 % current transmitting regime to a turbulent regime with a substantially lower transmitted current.

This study adds the secondary emission from the anode using a model with the energy and incident angle with the velocity distribution of the emitted electrons built in in order to study their effect on transmitted current. The secondary electrons emitted from the anode travel into the system against the electric field which subsequently turns them back to be re–collected at the anode. Hence, the secondary electrons have zero net contribution to the transmitted current but their charge adds to the space charge in the gap. The contribution of secondary electrons to the space charge depends upon the time they spend in the system which depends on their energy and the magnetic field they experience.

2 MX–1 Experiment

The MX-1 experiment ([9], [10]) was conducted to demonstrate the MINOS (Magnetically INsulating Opening Switch) concept [11] In this concept, the current in a cylindrical thermionic vacuum diode is controlled by an externally applied magnetic field. Thus, without magnetic field, the vacuum diode conducts current up the Child limit, and the switch is closed. When the applied magnetic field exceeds the Hull cut-off field, the electrons return to the cathode and no current is transmitted by the diode, i.e., the switch is open. The idealized voltage-current characteristic of a MINOS below cut-off is shown as the solid line in Figure 1, plotted using theory from Lau *et al.* [4] and Pollack [5] and verified in simulations by Verboncoeur and Birdsall [6]. The figure plots normalized transmitted current $p_n = J/J_C$ vs. normalized magnetic field $b_n = B/B_H$.

The experimental switch used a Ba-impregnated tungsten dispenser cathode with an area of 398 cm^2, and an OFHC polished copper anode. Anode-cathode gap sizes of 3 and 10 mm were used. With applied diode voltage, the diode current was monitored during the application of a time-varying magnetic field with dB/dt between $\approx 10^{-3}$ to 10^5 T/s. The results of these experiments are shown in Figure 1 as open squares for the 10 mm experiments and open circles for the 3 mm experiment. It should be noted here that the diode current was normalized to the measured diode current at B=0 (interpreted as the Child-Langmuir current with effective emitting cathode area $\geq 90\%$), and that the error bars are approximately $\pm$ 10 %, given by the uncertainty of the magnetic field amplitude in the small anode-cathode gap. (Similar error bars were obtained on the 10 mm experiments but are not shown to avoid crowding the plot). The 3mm data points represent experimental

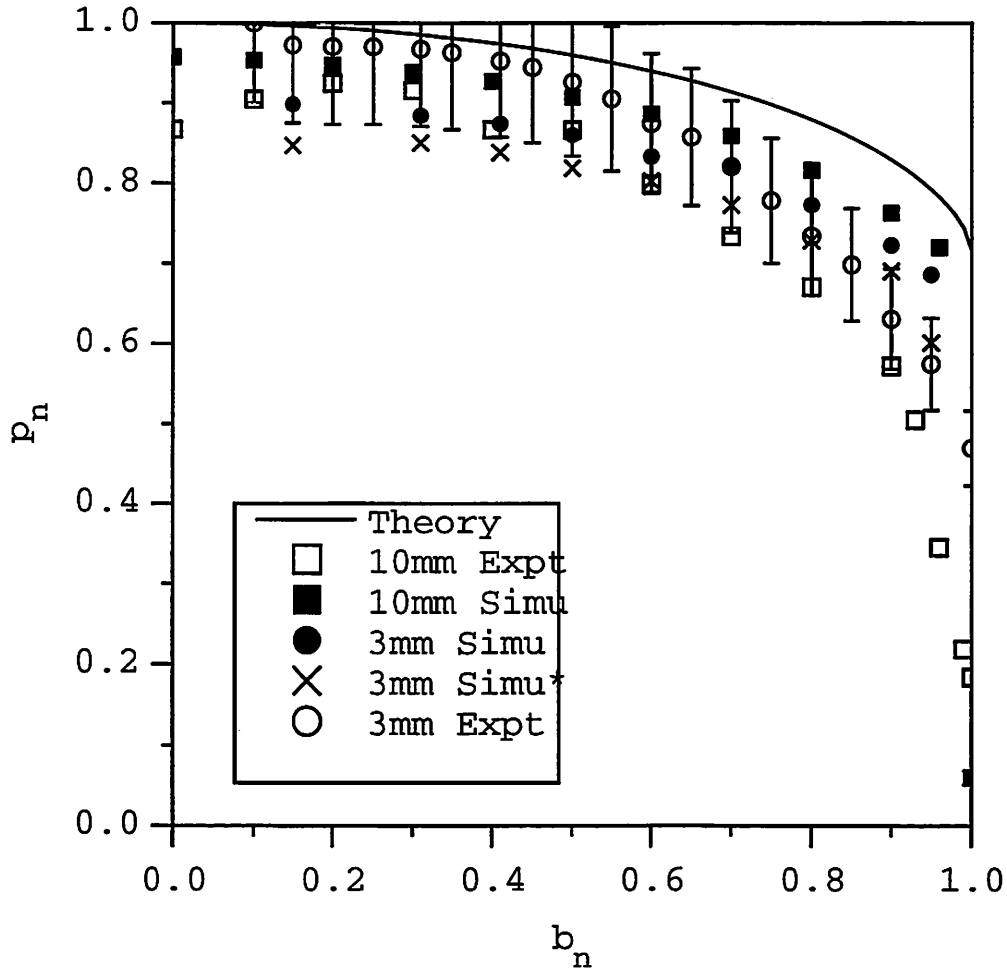

Figure 1: Comparison of normalized transmitted current (p_n) vs. normalized magnetic field (b_n) for PIC simulations with idealized theory and MX_1 experiments.

measurements done at a relatively lower bias voltage, ranging from 1kV at $b_n = 0$ to 1.6kV at $b_n = 1$. The 10mm data represent runs done at higher voltages of 2.2kV to 5.5kV for b_n between 0 and 1 respectively.

3 Discussion of Results

Simulations were done using the PIC code PDP1 [15] and the simulation model shown in Figure 2. Particles were emitted from the cathode at a given current density with a half Maxwellian distribution of thermal velocity 1×10^5 m/s (models a thermionic cathode at approximately 650^0 C). These (primary) electrons are then followed under the influence of the self consistent electric and applied magnetic fields. The electrons which reach the

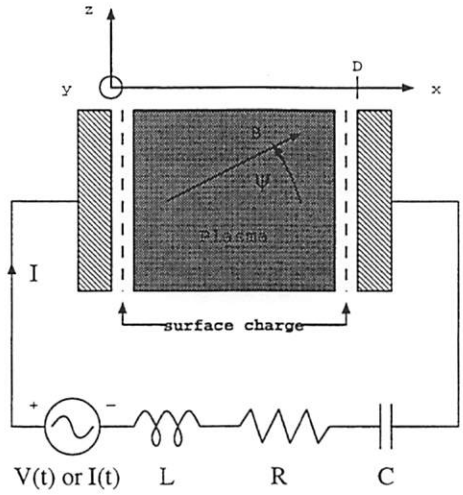

Figure 2: Simulations model.

anode create secondary electrons depending on their incident energy and their angle of incidence. The newly created secondaries were distributed in velocity space as described in the Appendix. The motions of these electrons are also treated self consistently in the total electric field all the particles. Some of the secondary electrons are actually reflected primaries (high energy) and will penetrate deeper and stay in the gap longer. Simulations were done using the current and voltage values obtained from the 3mm and 10mm experiments, assuming that the diode is in equilibrium at each of these points and therefore can be treated electro-statically. It should be noted here that due to the inductive nature of the MX–1 device's pulsing circuit, the gap magnetic field and voltage are **not** independent of each other. In fact the gap potential increases with increasing magnetic field as detailed in [10]. The normalization of current (i.e with $J_C = 2.336 \times 10^{-6} V_{gap}^{3/2}/D^2$) is done using the theoretical value of J_C at each of these points assuming no magnetic field, but that particular value of gap voltage. It should be noted here that while J_C and B_H scale simply with bias voltage, the secondary electron coefficient, σ, shows a highly nonlinear behavior with incident energy. This fact can often be hidden in normalized plots that plot details of experiments with different bias voltages on the same plot.

The results of the simulations runs are shown in Figure 1 labeled *3mm Simu*, *10mm Simu* and *3mm Simu**. The first two simulations were done for the 3mm and 10mm gap systems assuming anode material with a maximum secondary emission yield of 1.2, which is a typical value for a metal like stainless steel. The 3 mm Simu* points were done assuming a higher maximum secondary yield of 1.8 and a higher angular multiplier, k_s. Simulations

for the 10mm system with higher secondary emission coefficient did not show an appreciable change due to lower absolute yields at the higher voltages used for this case (see Appendix for details of secondary yield vs. energy) and hence are not shown. Simulations done without secondaries tracked the solid line theoretical curve Lau *et al.* [4] and simulations by Verboncoeur and Birdsall [7] closely and are not shown.

The point $b_n = 1$ is a highly sensitive point and even slight slight perturbation, (as a result of over–injection or secondaries) can drive the diode into a rapid current transition leading to a much lower transmitted current. The the behavior at $B = B_H$ has been discussed in detail by Verboncoeur and Birdsall [7] and for the cases shown simulated in Figure 1; the final normalized transmitted current does not appear to depend upon diode dimension or bias voltage. The points $b < b_n$ represent stable non-turbulent flow modes which exhibit reduced transmitted current due to the increased space charge from secondaries. The increase in space charge is highly dependent on the secondary yield for the lower voltage 3mm gap case as can be seen in the figure by the data points labeled *3mm Simu**.

In order to understand better the effect of secondaries on transmitted current, consider the set of plots representing density, the electric field and the gap potential, shown in Figures 3(a)–(c) respectively. The results shown in this figure are for a representative case of $b_n = 0.5$ for the 3mm diode. The solid lines in the sub–figures chart the variables at critical current without secondaries. i.e., these are the plots of the three variables when the diode is transmitting 100% of the injected current. This corresponds to the point ($p_n = 0.96$, $b_n = 0.5$) on the theoretical curve shown in Figure 1. The secondaries coefficients for this run were the same as that used for *3mm Simu** case.

Figure 3(a) shows the variation of density in the gap for the case with and without secondaries. In the absence of secondaries, as expected by theory, the electron number density shows a monotonic decrease from the cathode. The dashed line shows the result of the simulation with the same injection current as before, but with secondary emission turned on. As expected, the secondaries increase the space charge markedly near the anode. This is due to the large number of low energy secondaries that spend very little time in the diode. The charge density immediately in front of the cathode is higher than for the case without secondaries. Further, the total volume averaged charge is nearly 25% higher for the case with secondaries. In an earlier simulation, which had the reflected primaries emitted normal to the anode ($\theta = 0^o$), the E_x field showed a decided kink where these secondaries turned around at about $x = 7.5 \times 10^{-4}$m. The new secondary model (see Appendix) specularly reflects these electrons, so that some may reach the cathode.

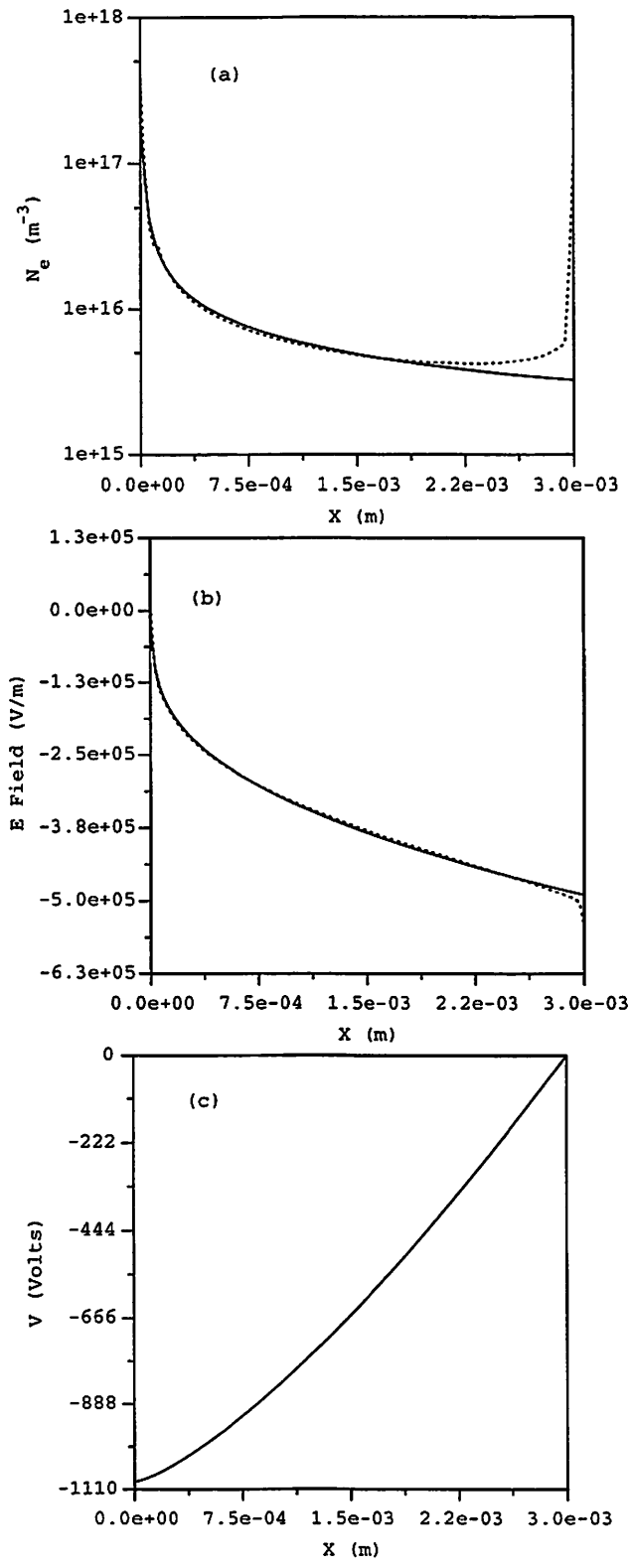

Figure 3: (a) Density, the corresponding electric field (b) and the potential in the gap (c) without (solid lines) and with (dashed) secondaries at $b_n = 0.5$

The effect of secondaries on the self–consistent electric field can be seen in Figure 3(b). The extra space charge right in front of the cathode leads to field reversal which turns back some of the injected primary electrons. The potential for the secondary case is slightly more negative in the gap indicating higher charge density. Since potential is obtained by twice integrating charge density, the behavior of the system apparent in the density plot is often masked in the potential plot. The overall effect of the extra charge leads to the reduction of transmitted current from 364.17 A ($p_n = 0.96$) to 296.1 A ($p_n = 0.813$), a decrease of over 15 %.

4 Conclusions

A computer experiment of the secondary electron emission model is presented and applied to the study of limiting current in crossed-field diodes. Secondaries are shown to reduce transmitted current. However, this effect is highly non–linear with respect to the applied voltage. Our studies show that the secondaries increase the overall charge in the gap, changing the electric field which reduces transmitted current. Simulations match some of the experimental trend partially. In particular, the reduction in transmitted current increases with increasing magnetic field. However, the simulations fail to model the larger decrease in transmitted current seen in the higher voltage 10mm gap case. It is highly unlikely that secondaries can cause this effect since yield at these energies is quite small (≈ 0.2). This is validated by simulations that used higher secondary emission yields with no appreciable change in transmitted current. Therefore, the present simulations show that secondaries can account for some of the reduction in current.

5 Acknowledgments

Thanks are due to Y. Y. Lau, D. Chernin, J. Swiegle and A. Shih for discussions on finer details of secondary emission properties. Thanks are also due to Peggy Christenson and John Verboncoeur for discussions on secondary emission model implementation and to Prof. C. K. Birdsall for advice and background on secondary and primary emission . This work was supported in part by the Office of Naval Research under Contract FD-N00014-90-J-1198 and AFOSR under grant F49620-92-J0487.

A Secondary Emission Model

A self-consistent secondary electron emission model is used in this study. This Appendix presents:

- Dependence of number of secondaries emitted on the primary electron energy.
- Change in number of secondaries emitted due to angle of incidence of primary electron.
- Velocity distribution of the emitted secondaries (speed and angle).

A.1 Energy Dependence

Figure A.1 shows a typical secondary electron yield vs. incident electron energy for a metal wall (note: yield can change from > 1 for a smooth surface to < 1 for a rough one). It can be seen that the yield peaks at an incident energy of approximately 500 V and then decreases steadily after that. This peak is due to the fact that a relatively low energy incidence electron may not dislodge the secondary while a relatively higher energy primary will be in contact with surface atoms for too short a time [12]. It is also of interest to note the two points E_1 and E_2 on Figure A.1, which are low and high energy points between which the yield of secondaries is greater than unity. Vaughan [13] has modeled this curve analytically

$$\sigma = \sigma_{max}(we^{1-w})^k \tag{A.1}$$

where

$$w = \frac{(E_i - E_0)}{(E_{max} - E_0)} \tag{A.2}$$

and E_0 is the minimum threshold energy, E_{max} is energy at maximum yield and σ_{max} is the corresponding yield. k is a curve fit parameter given by

$$\begin{aligned} k &= k_1 = 0.62 \text{ if } w \leq 1 \\ k &= k_2 = 0.25 \text{ if } w > 1. \end{aligned} \tag{A.3}$$

Shih *et. al* [14] have conducted experiments on polished molybdenum and find that the above theory shows good agreement with their results.

A.2 Angular Dependence

The secondary yield normally increases with the incidence angle (0^0 signifies normal incidence). The theory of variation of yield with incidence is described in [12] and more recently in [13] and [14]. An analytical model of angular dependence is presented in Vaughan [13]

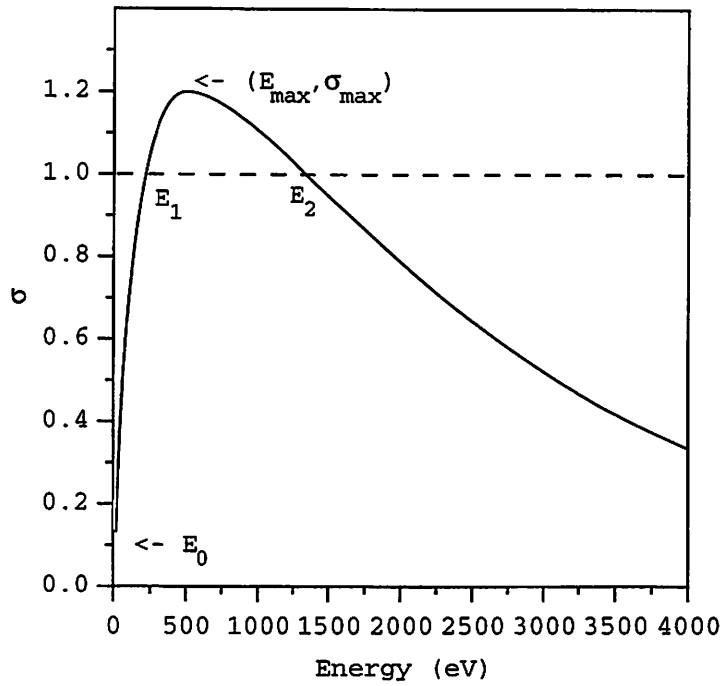

Figure A.1: A Typical Metal Secondary Yield vs. Incidence Energy Curve

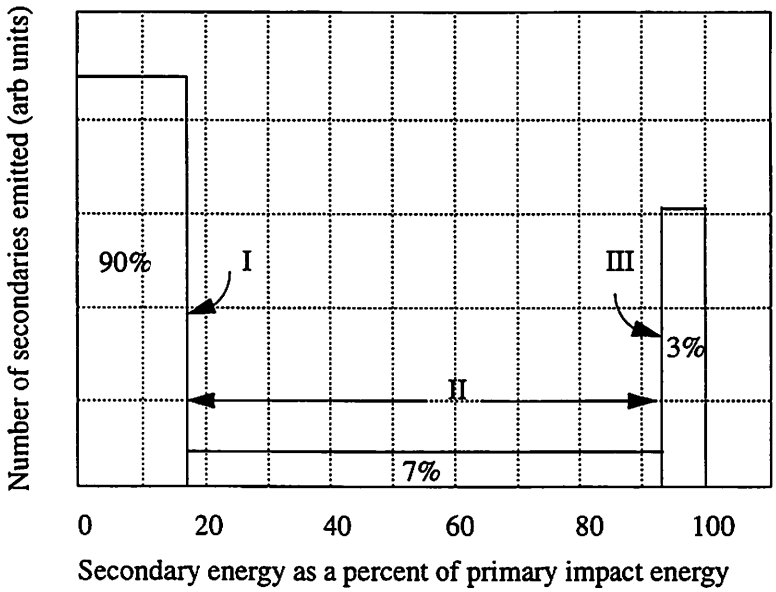

Figure A.2: Relative energy distribution of secondary electrons, adapted from Spangenberg [12] fig. 4.17, pg 52), as used in the simulation.

which accounts for the variation of E_{max} and σ_{max} with energy and adds a "smoothness" parameter k_s in order to model the characteristic of the surface. This model modifies the values of σ_{max} and E_{max} as

$$\sigma_{max\theta} = \sigma_{max0}(1 + k_s\theta^2/\pi) \tag{A.4}$$

and

$$E_{max\theta} = E_{max0}(1 + k_s\theta^2/2\pi) \tag{A.5}$$

to be used in equations (A.1) and (A.2). The value of k_s lies between 0 (rough) and 2 (smooth).

A.3 Secondary Velocity Distribution

There are few references available regarding the velocity spread of the emitted secondaries. Spangenberg [12] mentions that secondary electrons are emitted with an isotropic angular velocity distribution irrespective of the incident electron velocity spread. The energy distribution of the emitted electrons, shown in Figure A.2, includes:

- Low Energy (**I**) (true secondaries) 90% of the emitted electrons fall in this category with energies below 20 eV, peaking at around 10 eV. These are implemented in the simulation model by picking a random energy between 0-20 eV and then distributing them equally into the three velocity directions to provide an isotropic angular distribution.

- Medium Energy (**II**): 7% of the emitted particles lie in this energy range with energies ranging from 20 eV to 98% of the incident electron energy. The velocity distribution in the simulation is calculated the same way as in the low energy case.

- High Energy (**III**): (reflected primaries) These are not really secondary electrons but reflected primaries. 3% of the secondaries lie in this energy range which peaks around 99% of the incident electron energy. The reflected primary is assumed to be emitted specularly, i.e. the angle of reflection is equal to the angle of incidence. This is achieved by inverting the sign of v_x and keeping the signs of v_y and v_z the same.

References

[1] A. W. Hull, "The Effect of Uniform Magnetic Fields on the Motion of Electrons Between Coaxial Cylinders," *Phys. Rev* 18, 31 (1921).

[2] William G. Dow, *Fundamentals of Engineering Electronics*, John Wiley and Sons, New York, 1937

[3] C. K. Birdsall and W. B. Bridges, *Electron Dynamics of Diode Regions*, Academic Press, (1966).

[4] Y. Y. Lau, P. J. Christenson and D. Chernin, "Limiting Current in an Crossed-Field Gap," *Phys. Fl. I.5* 4486 (1993).

[5] M. A. Pollack, *Noise Transport in the Crossed-Field Diode*, Ph.D. thesis, University of California, Berkeley, CA, Series No. 60, Issue No. 485 (1962).

[6] J. P. Verboncoeur and C. K. Birdsall, "Simulations of Limiting Current in a Crossed-Field Gap, Hull Diode," presented at the IEEE ICOPS, Santa Fe, NM, June 1994.

[7] J. P. Verboncoeur and C. K. Birdsall. "Rapid current transition in a crossed-field diode," Phys. Plasmas **3** 3, March 1996.

[8] B. H. Vanderberg and J. E. Eninger, "Space-charge limited current cut-off in crossed fields," Phys. Plasmas **3** 3, Feb 1997.

[9] B.H.Vanderberg and J.E.Eninger, "Parametric Scaling Study of a Magnetically Insulated Thermionic Vacuum Switch" IEEE Trans. Plasma Sci. 24 (1), 165 (1996).

[10] B. H. Vanderberg *Experimental and Analytical Study of a Magnetically Controlled Thermionic Vacuum Switch Concept*, Doctoral Thesis, Dept. of Industrial Electrotechnology, Royal Institute of Technology, Sweden, 1994.

[11] J.E.Eninger, "MINOS - A High Power Opening Switch Concept", Bullet. Am. Phys. Soc. 29, 1342 (1984).

[12] Karl R. Spangenberg, *Vacuum Tubes*, McGraw-Hill, New York, 1948

[13] J. R. M. Vaughan, "A New Formula for Secondary Emission Yield," IEEE Trans. **ED-36**, 1963 (1989).

[14] A. Shih and C. Hor, "Secondary Emission Properties as a Function of the Electron Incidence Angle" IEEE Trans. **ED-40**, 824 (1993).

[15] J. P. Verboncoeur, V. Vahedi, M. V. Alves and C. K. Birdsall, *PDP1, PDC1 and PDS1: Plasma Device one-dimensional Bounded Electrostatic Codes,* Plasma Theory and Simulation Group,University of California, Berkeley, CA 94720. Available via *http://ptsg.eecs.berkeley.edu.*